Trace species detection in the near infrared using Fourier transform broadband cavity enhanced absorption spectroscopy: initial studies on potential breath analytes

W. Denzer[1,2], G. Hancock[1], M. Islam[3], C. E. Langley[1], R. Peverall[1†], G. A. D. Ritchie[1], D. Taylor[1]

[1] Department of Chemistry, Physical and Theoretical Chemistry Laboratory, University of Oxford, South Parks Road. Oxford OX1 3QZ, UK
[2] Oxford Medical Diagnostics Ltd, Oxford University Begbroke Science Park, Sandy Lane, Yarnton, Oxford OX5 1PF, UK
[3] School of Science and Technology, University of Teesside, Borough Road, Middlesbrough TS1 3BA, UK

[†]Email: Robert.Peverall@chem.ox.ac.uk

Abstract

Cavity enhanced absorption measurements have been made of several species that absorb light between 1.5 and 1.7 μm using both a supercontinuum source and superluminescent light emitting diodes. A system based upon an optical enhancement cavity of relatively high finesse, consisting of mirrors of reflectivity ~ 99.98%, and a Fourier transform spectrometer, is demonstrated. Spectra are recorded of isoprene, butadiene, acetone and methane, highlighting problems with spectral interference and unambiguous concentration determinations. Initial results are presented of acetone within a breath-like matrix indicating ppm precision at < ~10 ppm acetone levels. Instrument sensitivities are sufficiently enhanced enabling the detection of atmospheric levels of methane. Higher detection sensitivities are achieved using the supercontinuum source, with a minimum detectable absorption coefficient of ~ 4×10^{-9} cm^{-1} reported within a 4 minute acquisition time. Finally, two superluminescent light emitting diodes are coupled together to increase wavelength coverage, and measurements made simultaneously on acetylene, CO_2, and butadiene. The absorption cross sections for acetone and isoprene have been measured with an instrumental resolution of 4 cm^{-1} and are found to be $1.3 \pm 0.1 \times 10^{-21}$ cm^2 at a wavelength 1671.9 nm and $3.6 \pm 0.2 \times 10^{-21}$ cm^2 at 1624.7 nm, respectively.

Introduction

The desirable ability to make high sensitivity measurements across a broad spectral region has led to recent developments in broad-band cavity enhanced absorption spectroscopy (BB-CEAS) [1-17]. There are clear advantages in having this capability: to measure several compounds simultaneously and to increase the amount of information in a particular measurement, thereby statistically enhancing the output (for example, in measuring several spectral lines to record an isotopic ratio); and to improve specificity, where target species exhibit relatively broad spectral signatures. Several schemes have been reported for BB-CEAS involving different sources and detection apparatus, and including application to the measurement of liquid and/or surface borne species [10,13,14,15,18,19]. On the whole, these studies have been at visible wavelengths, and as broad band optical sources both light emitting diodes and discharge lamps have featured predominantly and have been used with either imaging spectrometers or Fourier transform interferometers as detection systems. Relatively high resolution is possible when desirable (0.05 cm^{-1} is reported in [5]) but broad-band acquisition comes at the cost of time if sensitivity is to be maintained. Many of the applications for BB-CEAS reported have involved the atmospheric measurement of species such as the oxides of nitrogen which at visible wavelengths lend themselves well for detection by this technique as they invariably exhibit broad spectral features. The sensitivities that have been demonstrated have tended to be in the 10^{-9} cm^{-1}

range, for systems using mirrors of relatively high reflectivity (as high as R = 99.995 % has been demonstrated [8]) and for acquisition times of several minutes. Recently, applications of high power supercontinuum sources have been reported [20,21] including one utilising broad band retroreflective prisms [20]. Supercontinuum sources are unique in their ability to produce several Watts of (usually pulsed) radiation across a wavelength range stretching from the blue to the near infrared, and therefore constitute an ideal, but relatively expensive tool for BB-CEAS experiments. Similarly, femtosecond lasers, used to produce frequency combs have also been demonstrated with this technique [3,22,23] and have shown extremely good sensitivity and bandwidth but with technically demanding detection schemes (see for example [24]).

An earlier study from this laboratory [25] demonstrated the principles of near infrared BB-CEAS using a superluminescent light emitting diode (SLED), a source with a relatively high spectral power density and spatial coherence. Preliminary data were shown using butadiene as a test molecule absorbing SLED radiation between ~1.6 and ~1.7 μm, a spectral region where many hydrocarbons exhibit overtone and combination band absorptions. The work presented here expands on this by employing both a supercontinuum (SC) source and a combination of SLEDs to measure samples containing several species, and constitutes some of the first measurements recorded using this technique in this wavelength range. The sensitivities achievable are reported, and a critique is made of the technique's response to mixtures where overlapping absorptions exist between different molecules. The specific target molecules that have been chosen are isoprene, acetone, butadiene and methane. These compounds are potentially important as markers of disease and/or because of their toxicology, or they may well represent potential interference in the successful measurement of any one of the other molecules. Mixtures of acetone with isoprene are analysed, simulating possible levels that may occur in human breath, and the response of the instrument to simultaneous absorption by broad- and narrow-band absorbers is demonstrated with mixtures of acetone and breath. The versatility of the SLED, a cost effective light source, is demonstrated in measurements of different species over a wide spectral range (750 cm-1).

Experiment and methodology

The experimental arrangement is similar to that used in our previous study [25] and differs essentially in only two aspects: firstly, only a Fourier transform interferometer is used for detection; and secondly, a supercontinuum source is demonstrated as well as SLED sources. An experimental schematic is illustrated in figure 1 showing both SC source and SLED source beam paths, which are not used simultaneously. The SC source is a Fianium SC450-4 (UK), producing in total 4 W of power across a spectral range spanning from 450 nm to 2.5 μm. Output from the SC source is not continuous, but is pulsed at 40 MHz (ps pulse length)[16]. For spectroscopic measurements in the region of interest (around 1.65 μm) the SC output is passed through two filters (Thorlabs FEL1500 edgepass and bk interferenzoptik bandpass bk-1655-60-B (centred around 1655 nm with a 60 nm bandwidth)) confining the wavelengths that enter the FTIR to between ~1.6 – 1.7 μm: this is crucially within the stop band of the high reflectivity cavity mirrors, so as not to saturate the detector. The optical power from the SC source within this spectral range and directed upon the cavity is ~40 mW, and for adequate stability the SC source must be operated at full power for several (2 – 3) hrs before measurements are taken. The optical enhancement cavity consists of two high reflectivity mirrors (Research Electro-Optic, R ~ 99.98 %, 1.5μm < λ < 1.7μm, radii of curvature 1.5 m) confined within a vacuum vessel and separated by 25 cm. The initial alignment of the optical cavity is carried out with a diode laser which is co-aligned with the optical beam path of the broad-band sources. Light exiting the cavity is directed through a convex lens (focal length 25 cm) and straight into the FTIR and onto the detector (Thorlabs InGaAs DET410) that resides within the FTIR sample compartment. For experiments employing two SLEDs of central wavelengths 1550 nm (Covega) and 1650 nm (DenseLight Semiconductors) the beams are merged using a polarising beam-splitter and directed towards the cavity and FTIR. The total optical power incident on the cavity was ~ 10 mW. The combined optical emission from the

SLEDs is shown as an inset in figure 5. No optical filters are required with the SLEDs as the emission is limited to within the mirror stop-band.

Samples of isoprene, butadiene, acetone (all Sigma-Aldrich), acetylene, CO_2, (BOC) and methane (BOC and CK gas products Ltd), and several mixtures of these substances are used in this study. Dilute samples of liquid vapour are made by mixing a known quantity of vapour within a cell connected to a vacuum line and buffering the cell with air. Liquid samples are first frozen and pumped upon for several minutes to remove impurities, and because of the tendency for liquid samples to condense on any surfaces the pressure is allowed to equilibrate and stabilise. Nevertheless, we recognise that some uncertainty in the actual concentration of sample exists within the buffered holding cell, and further unavoidable uncertainties are introduced when any of the sample is transferred into the cell containing the optical cavity. Despite these potential problems with sample handling, our cavity enhanced optical absorption measurements always return signals within reasonable bounds of that which is expected (within ~ 20%), and act as a double check on the gas handling procedures. Necessarily, the uncertainties that arise from these issues are propagated through to any quoted results (unless otherwise stated), but they do little to influence the following discussions. Gaseous samples are used without further purification.

Sample spectra are taken at various pressures as monitored with a capacitance manometer (Leybold Piezovac), and are initially processed within the FTIR (i.e. acquiring and processing the interferogram). Baseline spectra are acquired by evacuating the optical cell before and after each set of measurements, and the cavity enhanced absorption spectra are obtained by treating the data according to the following equation [26]:

$$\frac{(I_0 - I)}{I} = \frac{\alpha L}{1 - R}. \qquad \text{Equation 1}$$

where, I and I_0 are the recorded cavity enhanced signals with and without the presence of absorbing sample, respectively, α is the absorption coefficient, L is the physical pathlength and $R(\lambda)$ is the geometric mean of the mirrors' reflectivities. The wavelength dependent geometric mean $R(\lambda)$ is ascertained by comparing standard spectra of species (particularly butadiene and methane) with the cavity enhanced spectra, as in [25], and at the different instrument resolutions (predominantly 4 cm^{-1} and 16 cm^{-1}) used here.

Results and discussion

Broadband cavity enhanced spectra taken using the SC source, of isoprene, acetone and methane are shown in figure 2(A-C). As a consequence of its structural similarity with butadiene, isoprene exhibits a very similar spectral fingerprint to butadiene, especially at the low resolution (16 cm^{-1}) in figure 2(A). The overtone and combination spectrum of acetone in this region results from excitation of the in-plane (ν_3) and out-of-plane (ν_1, ν_2) CH oscillators described by the notation $|\nu_1\nu_2\rangle_{+/-}|\nu_3\rangle$ according to Kjaergaard et al.[27]. A single sharper feature is observed in the spectrum of acetone (near 1672 nm), apparent at higher resolution, which is coincident with the $|10\rangle_{+/-}|1\rangle$ modes as described in [27]. The peak centred at 1690 nm is assigned as the $|11\rangle|0\rangle$ mode in the same reference. All of these spectra have been corrected for the mirror reflectivity $R(\lambda)$. The methane spectra are shown at a resolution of 4 cm^{-1} for three different samples: two calibration mixtures containing 7.5 and 15 ppm of methane in dry air, and a third of laboratory air containing ~1.8 ppm of methane. The dominant feature in the methane spectrum at 1665 nm is the spectrally congested Q-branch of the $2\nu_3$ overtone, and even at the comparatively low resolution (compared to the pressure broadened methane linewidths encountered in this region) methane produces an easily recognisable spectrum at atmospheric levels.

The measured cross section for acetone for the peak absorption at 1671.9 nm (5981 cm^{-1}) is 1.3 ± 0.1 × 10^{-21} cm^2 as recorded with an instrumental resolution of 4 cm^{-1}; the absolute cross section may thus be

slightly higher than this as this resolution leads to a slight broadening of this spectral feature. This measurement is in good agreement with that of Wang et al. (2004) [28] who report 1.2×10^{-21} cm^2 at 6000 cm^{-1}. The peak isoprene cross section is higher reaching a maximum of $3.6 \pm 0.2 \times 10^{-21}$ cm^2 at 1624.7 nm (6155 cm^{-1}). Measurements by Cias et al. [29] of the isoprene cross section at 1651.52 nm yield a value ~ 11 times smaller than this, in keeping with the relative sizes of the absorption at the two different wavelengths (both these experiments use diode lasers).

The sensitivity of this technique was gauged by repetitively recording successive background (I_0) signals (over ~ 0.5 hrs) and treating some as 'I' as set out in equation 1. The minimum detectable absorption is then determined from the standard deviation of the blank. This is done for different combinations of datasets representing I and I_0 to arrive at a typical value for the standard deviation of the blank. In principle this method leads to a more realistic value for the minimum detectable absorption, than for example just determining the noise level on a particular dataset from a broadband absorber, as it also reflects to a certain extent the stability of the system. For the SLED measurements, sensitivities expressed as a minimum detectable absorption coefficient of $\alpha_{min} \sim 2 \times 10^{-8}$ cm^{-1} are obtained, in keeping with our previous results using the same cell and mirror set [25]. However, for the SC source experiments we see an improvement in sensitivity, such that α_{min} is reduced to $\sim 5 \times 10^{-9}$ cm^{-1}. (We note that actual values of α_{min} vary between 1.5 – 2.3×10^{-8} cm^{-1} and $4 – 6 \times 10^{-9}$ cm^{-1} between 1.6 and 1.7 μm for the SLED and SC source, respectively, as a consequence of $R(\lambda)$, and that due to uncertainties in the determination of R there is a 10% error on these values.) The power incident on the cavity is only four times greater for the SC source compared to the SLED, and therefore the sensitivity improvement cannot be due to this alone. While we can speculate that the remaining difference is perhaps a result of some residual coherence in the cw SLED that leads to interference noise, or possibly a slight susceptibility to optical feedback leading to amplitude noise, it could also be due to other factors such as a serendipitous advantageous alignment that is difficult to optimise at this level, or an approach of the noise floor of the detection apparatus; we feel however, that it is unlikely to be the former, as this effect seems reproducible over several misalignment – realignment operations when swapping between SC source and SLED source.

The sensitivities quoted here have been achieved for instrument resolutions of both 4 cm^{-1} and 16 cm^{-1}, and an acquisition time of 4 minutes and while they give a good guide to the applicability of the technique, and a suitable value with which to compare to other techniques (that are judged very much in the same way), we note that for high confidence (90 %) quantitation an absorption level of ~ 10 times higher than this sensitivity is desirable. The sensitivity obtained in these experiments is amongst the highest reported, when compared to other BB-CEAS studies. Venables et al. [4] report the highest sensitivity of 5×10^{-10} cm^{-1}, in an incoherent BB-CEAS study (over a 60 s acquisition time) for the detection of NO_3 around 660 nm. This is ~ 10 times better than the sensitivity reported here, but this has been achieved using an optical cavity of physical length 4.5 m (some 18 times longer than that used in this study). The direct comparison of these numbers should however be undertaken with caution, as there are certain parameters that are not always easily determinable, and others that are not reported, but required to make a fair comparison. Partly, this comparison has been made to put this work into context, but it may also highlight advantages and disadvantages of different methodological configurations. The resolution that has been chosen here reflects the 'shape' of the spectral signatures of the target species such as acetone and isoprene that on the whole are featureless on the 1 cm^{-1} scale. Increasing the resolution beyond this will lead to a reduction in signal/noise (the S/N ratio) for these species for measurements taken over equivalent acquisition times, but may well lead to a slight increase in S/N for the narrow band absorbers such as CO_2, CH_4 and H_2O. It is worth noting that, at least in terms of resolution, any such experiment of this sort can be optimally configured depending upon the target species. Furthermore, the simulation of FTIR data is a mature field and can be undertaken regardless of whether the resolution (and instrument function) surpasses typical linewidths or not.

Key issues in any method for detecting multiple species are that of interference and non-specificity.

In mass spectrometry these are enduring problems, especially in single stage devices, and these are somewhat alleviated by, for example, implementations of gas chromatography – mass spectrometry (GCMS). Aside from the possibility of absolute measurements, the benefit of a spectroscopic tool for molecular identification is that on the whole specificity is guaranteed, as most molecules have a unique spectral signature. The caveat to this is that similar signatures can result from similar molecules, but they are never exactly the same. However, for any given spectroscopic instrument, the bandwidth within which spectral signatures occur can be rather narrow and therefore there is a tendency for overlapping signatures and congestion, in other words, spectral interference. This can have an adverse effect in the positive identification of a particular species. A particularly bad example of this is in the identification of either isoprene or butadiene in the presence of similar quantities of the other (or if the relative quantities are unknown).

In human breath, isoprene, acetone and methane are all present to a certain extent, and absorb radiation in roughly the same spectral region. Levels of isoprene have been reported at ~ 200 ppb [30,31], while those of acetone and methane can reach tens of ppm, depending upon the condition of the subject [31-35]. To simulate the relative concentrations possible in breath of isoprene and acetone, a mixture was made of 0.5 % of isoprene and 5 % acetone, buffered in air. This mixture was analysed at a reduced pressure in the cavity enhanced cell, diluting the sample further with air to achieve ppm levels of acetone. The results are shown in figure 3. Clearly, despite some overlap between isoprene and acetone absorption, the two species are clearly discernable, with acetone easily identifiable at the 10 ppm level. Note that there is not enough atmospheric methane present at these reduced pressures for it to register in the spectra. Finally a breath sample from a healthy volunteer has been analysed, showing only relatively weak background absorption (figure 4), predominantly from CO_2, methane and water, suggesting that this spectral region is an attractive one, especially for detection of acetone; the only potential drawback being the relatively low acetone absorption cross sections. Figure 4 also includes a simulation of the breath spectrum using readily available spectral information from the Hitran database **[**36**]**; on the whole the simulation is accurate, but with some discrepancy at longer wavelengths where both light intensity is limited and the mirror reflectivity is dropping. A spectrum of a mixture of a 25 ppm acetone/dry air sample and breath is also reported and is shown offset for clarity in figure 4. Due to dilution, the proportion of acetone in this mixture should be ~ 10 ppm and the presence of acetone is clearly apparent. Including the acetone cross sections in a fit to this data returned a concentration value of 7.3 ± 1.3 ppm (note this is the error only from the fit). We expect this number will become more precise as we refine the simulation data; the low value of 7.3 ppm could be the result of several ambiguities, not least the amount of acetone in the original sample: a similar fit to one atmosphere of the undiluted 25 ppm acetone/air mix (but obviously excluding the CO_2 and water) yielded a value of ~21 ppm. Part of this discrepancy could lie in the uncertainty of $R(\lambda)$ (about 2 – 3 ppm), but this also highlights issues when handling and producing samples containing substances such as acetone. As stated earlier in the text, from experience of handling vapour samples, we anticipate only to be within ~20 % of expected values and we presume similar uncertainties will exist in handling the pre-prepared acetone mixture (not just our sample handing but also that of the supplier). We note that the sample cell in these experiments is only 25 cm long, and thus an improvement to detecting acetone possibly to sub-ppm levels could be achieved merely by lengthening the cell. Clearly the presence of the CO_2 absorption would make it difficult to unambiguously determine breath isoprene concentrations in this spectral region, and we would have to consider the possibility of pre-concentration/separation techniques in order to achieve this.

Example data of a mixture of three molecular species buffered in air from the dual SLED experiment are shown in figure 5 together with the combined spectral output of the two SLEDs (see inset in figure 5). Between the two SLED emission profiles, at around 1600 nm, the intensity of the light is very low and subsequently the noise level in the spectrum is large, but in essence the broadband source covers ~ 750 cm^{-1}. Thus the scan range is about the same as the stop band of the high reflectivity mirrors, at least where the mirrors are at their most reflective (R > 99.95 %). Coupling together more SLED sources to increase the

wavelength range in this case would therefore be unproductive (except to increase the light intensity), unless high reflectivity mirrors with a broader response could be found. However, generally there are limits to the spectral coverage of high reflectivity dielectric mirrors (usually ~200 nm in the near IR), although there is perhaps potential to extend this with promising coating technologies such as sub-wavelength gratings [37], but these have yet to be demonstrated at the high reflectivity required for this work. One possible alternative to dielectric coatings is to use prism retroreflectors based on total internal reflection [20,38] which promise unprecedented wavelength coverage, but require stringent specifications as a consequence of surface scattering and bulk material absorption/scattering ($10^{-3}\lambda$ super polishing and high quality material is required). In Figure 5, both acetylene and CO_2, which at high resolution have relatively uncongested spectra show only broad absorption features here because of the low instrumental resolution (16 cm^{-1}).

Conclusions

Both SC and coupled SLED sources have been demonstrated to work effectively with BB-CEAS in the NIR. With the former, issues surrounding the implementation of such a broadly emissive source must be circumvented to limit the wavelength coverage to the stop band of the high reflectivity mirrors, and so prevent detector saturation. With this achieved, data acquired with the SC source show the higher sensitivity ($\alpha_{min} \sim 4 \times 10^{-9}$ cm^{-1}). Nevertheless the SLED sources are versatile and cost effective, and as shown here can be easily coupled together to increase the wavelength range. Samples containing mixtures of gases have been analysed with a view to testing the response of the apparatus in more real-life analytical scenarios. Results indicate that such a device is capable of unambiguously determining analytes such as acetone in a human breath matrix to ppm levels. However, a simulation of the data is required which must necessarily accurately represent the instrument's response to all the interferands. Furthermore, the behaviour of the spectrometer must be judged across a wide range of sample conditions that may be experienced in human breath (especially variations in acetone, methane, carbon dioxide and water) in order to properly determine the statistics of the outcome of the target species measurement.

Acknowledgements

The authors would like to thank the EPSRC for financial support of this project, including an advanced research fellowship (RP) and a case award in association with SEEDA (CEL).

[1] S. E. Fiedler, A. Hese and A. A. Ruth, *Chem. Phys. Lett*., 2003, **371**, 284.
[2] S. E. Fiedler, G. Hoheisel, A. A. Ruth and A. Hese, *Chem. Phys. Lett.*, 2003, **382**, 447.
[3] T. Gherman, S. Kassi. A. Campargue, D. Romanini, Chem. Phys. Letts, 2004, **383**(3-4), 353.
[4] D. S. Venables, T. Gherman, J. Orphal, J. C. Wenger and A. A. Ruth, *Environ. Sci. Technol*., 2006, **40**(21), 6758.
[5] A. A. Ruth, J. Orphal and S. E. Fiedler, *Appl. Opt*., 2007, **46**(17),3611.
[6] S. Vaughan, T. Gherman, A. A. Ruth and J. Orphal, *Phys. Chem.Chem. Phys*., 2008, **10**, 4471.
[7] J. Orphal and A. A. Ruth, *Opt. Express*, 2008, **16**(23), 19232.
[8] S.M. Ball, J. M. Langridge and R. L. Jones, *Chem. Phys. Lett*., 2004,**398**, 68.
[9] J. M. Langridge, S. M. Ball and R. L. Jones, *Analyst*, 2006, **131**, 916.
[10] M. Islam, L. N. Seetohul and Z. Ali, *Appl. Spectrosc*., 2007, **61**(6),649.
[11] J. M. Langridge, S. M. Ball, A. J. L. Shillings and R. L. Jones, *Rev. Sci. Instrum*., 2008, **79**, 123110.
[12] M. Triki, P. Cermak, G. Mejean and D. Romanini, *Appl. Phys. B:Lasers Opt*., 2008, **91**, 195.
[13] L. N. Seetohul, Z. Ali and M. Islam, *Anal. Chem*., 2009, **81**(10),4106.
[14] L. N. Seetohul, Z. Ali and M. Islam, *Analyst*, 2009, **134**, 1887.
[15] A. A. Ruth, K. T. Lynch, *Phys. Chem. Chem. Phys*. 2008, **10**(47), 7098.
[16] J. M. Langridge, T. Laurila, R. S. Watt, R. L. Jones, C. F. Kaminski and J. Hult, *Opt. Express*, 2008, **16**(14), 10178.
[17] M. Schnippering, P. R. Unwin, J. Hult, T. Laurila, C. F. Kaminski, J. M. Langridge, R. L. Jones, M. Mazurenka and S. R. Mackenzie, *Electrochem. Commun*., 2008, **10**(12), 1827.
[18] L. van der Sneppen, G. Hancock, C Kaminski, T. Laurila, SR Mackenzie, SRT Neil, R Peverall, GAD Ritchie, M

Schnippering, PR Unwin, *Analyst*, 2010, **135**, 133.
[19] S. S. Kiwanuka, T. Laurila, C.F. Kaminski, *Analytical Chemistry* 2010, **82**(17), 7498.
[20] P. S. Johnston, K. K. Lehmann, *Opt. Express*, 2008, **16**(19), 15015
[21] R. S. Watt, T. Laurila, C. F. Kaminski, et al. *Appl. Spectrosc*. 2009, **63**(12), 1389.
[22] M. J. Thorpe, D. Balslev-Clausen, M. S. Kirchner, J. Ye, *Opt. Express*, 2008, **16**(4), 2387.
[23] M. J. Thorpe, J. Ye, *Appl. Phys. B*, 2008, **9**1(3-4), 397.
[24] B. Bernhardt, A. Ozawa, P. Jacquet, M. Jacquey *et al. Nature Photon*. 2010, **4**(1), 55.
[25] W. Denzer, M.L. Hamilton, G. Hancock, M. Islam, C.E. Langley, R. Peverall, G.A.D. Ritchie, *Analyst*, 2009, **134**, 2220.
[26] M. Mazurenka, A. J. Orr-Ewing, R. Peverall and G. A. D. Ritchie, *Annu. Rep. Prog. Chem*., Sect. C, 2005, **101**, 100.
[27] H.G. Kjaergaard, B.R. Henry, A.W. Tarr, *J. Chem. Phys*., 1991, **94**(9) 5844.
[28] C. J. Wang, S. T. Scherrer, D. Hossain, *Appl. Spectros*. 2004, **58**(7), p784.
[29] P. Cias, C. J. Wang, T. S. Dibble, *Appl. Spectros.* 2007, **61**(2) p 230.
[30] I. Kushch, B. Arendacka, S. Stolc, P. Mochalski, W. Filipiak, K. Schwarz, L. Schwentner, A. Schmid, A. Dzien, M. Lechleitner, V. Witkovsky, W. Miekisch, J. Schubert, K. Unterkofler, A. Amann, *Clinical Chemistry and Laboratory Medicine,* 2008, **46**(7), 1011.
[31] M. Kinoyama, H. Nitta, A. Watanabe, H. Ueda, *Journal of Health Science*, 2008, **54**(4), 471.
[32] C.J. Wang, A. Mbi, M. Shepherd, *IEEE Sensors Journal*, 2010, **10**(1), 54.
[33] C.H. Deng, J. Zhang, X.F. Xu, W. Zhang, X.M. Zhang, *Journal of Chromatography B-Analytical Technologies in the Biomedical and Life Sciences*, 2004, **810**(2), 269.
[34] C. Wang, P. Sahay, *Sensors*, 2009, **9**, 8230-8262
[35] C. Turner, C. Walton, S. Hoashi, M. Evans, *J. Breath Res.* 2009, **3**(4) art. 046004
[36] L. S. Rothman, I. E. Gordon , A. Barbe, D. Chris Benner, P. F. Bernath, et al. *J. Quant. Spectros. Rad. Trans*. 2009, **110**, 533.
[37] L. Chen, M.C.Y. Huang, C.F.R. Mateus, C.J. Chang-Hasnain, Y. Suzuki, *Appl. Phys. Lett*., 2006, **88**(3), 031102
[38] K.K. Lehmann, P.S. Johnston, P. Rabinowitz, *Appl. Opt.* 2009, 48(16), 2966.

Figure captions

Figure 1. Experimental arrangement showing both the supercontinuum light source (SC) and the dual SLED beam paths. The polarisations of the light from each of the SLED devices are arranged to be mutually perpendicular, and so the beams can be merged efficiently using a polarising beamsplitter. Light is directed into the optical cavity formed by mirrors M_1 and M_2 and thereafter into an FTIR.

Figure 2. A)The spectrum of isoprene acquired with an FTIR resolution of 16 cm^{-1}. The samples analysed are a 1in 100 dilution of isoprene in air at the quoted total pressures. B) Spectra taken at different quoted pressures of a 1 in 50 dilution of acetone in air recorded over 4 minutes with the SC source and at a resolution of 0.5 cm^{-1}. C) Spectra acquired of 1-atmosphere air samples containing different quantities of methane, including a sample of laboratory air which has approximately 1.8 ppm methane. The FTIR resolution was set to 4 cm^{-1}.All the spectra have been corrected for $R(\lambda)$ and were acquire over 4 minutes using the SC source.

Figure 3. Spectra of a mixture of isoprene and acetone in the ratio ~ 1:10 to simulate potential relative breath concentrations. Measurements have been made of the mixture in a bath gas of air at a total pressure of 50 Torr. The effective acetone concentrations are quoted calculated from the partial pressure of acetone relative to one atmosphere. The resolution of the FTIR is 4 cm^{-1}.

Figure 4. The spectrum of the breath of a healthy volunteer (solid black line) at atmospheric pressure, showing CO_2, methane and water. The simulation (dashed red line) uses cross section data from the Hitran database [30] convolved with a Gaussian instrument function to match the FTIR

resolution of 4 cm^{-1}. The partial pressures in the simulation are 28Torr, 7 Torr and 2.4 mTorr for CO_2, water and methane, respectively. Offset (upper curve) is a spectrum of a mixture of breath with an acetone sample (see text) such that there is ~10 ppm acetone (total pressure also 1 atm).

Figure 5 Data recorded over 4 minutes using the dual SLED arrangement between 1500 nm and 1700 nm of a mixture of acetylene (3 %), CO_2 (30 %) and butadiene (0.5 %) in air (66.5 %) at the total pressures quoted and at an instrument resolution of 16 cm^{-1}. The inset shows the combined intensity of the two SLEDs.

Figure 1

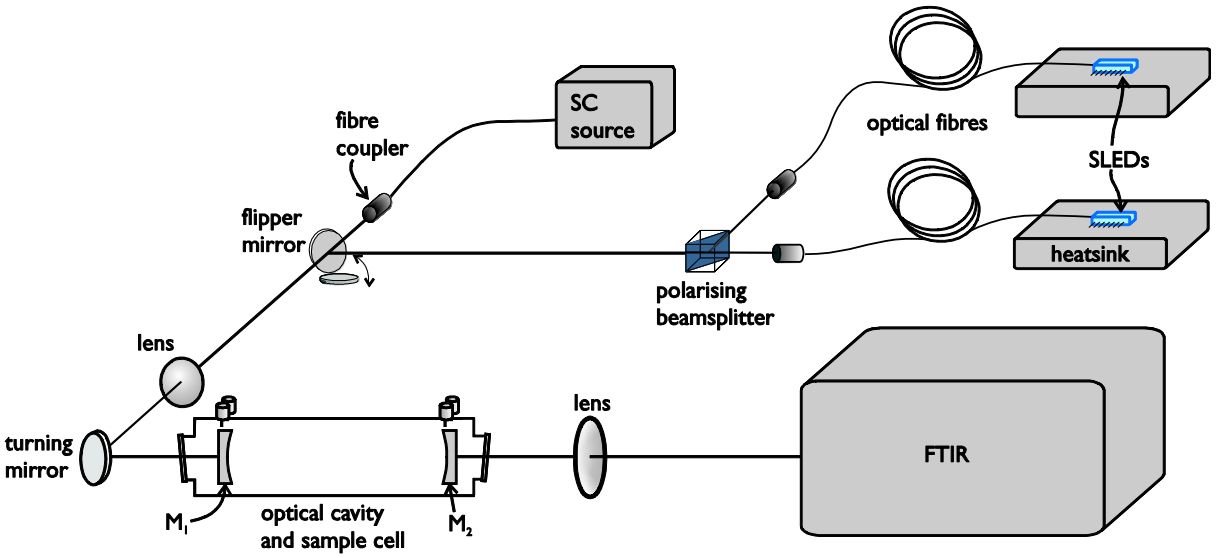

Figure 2 A, B, C

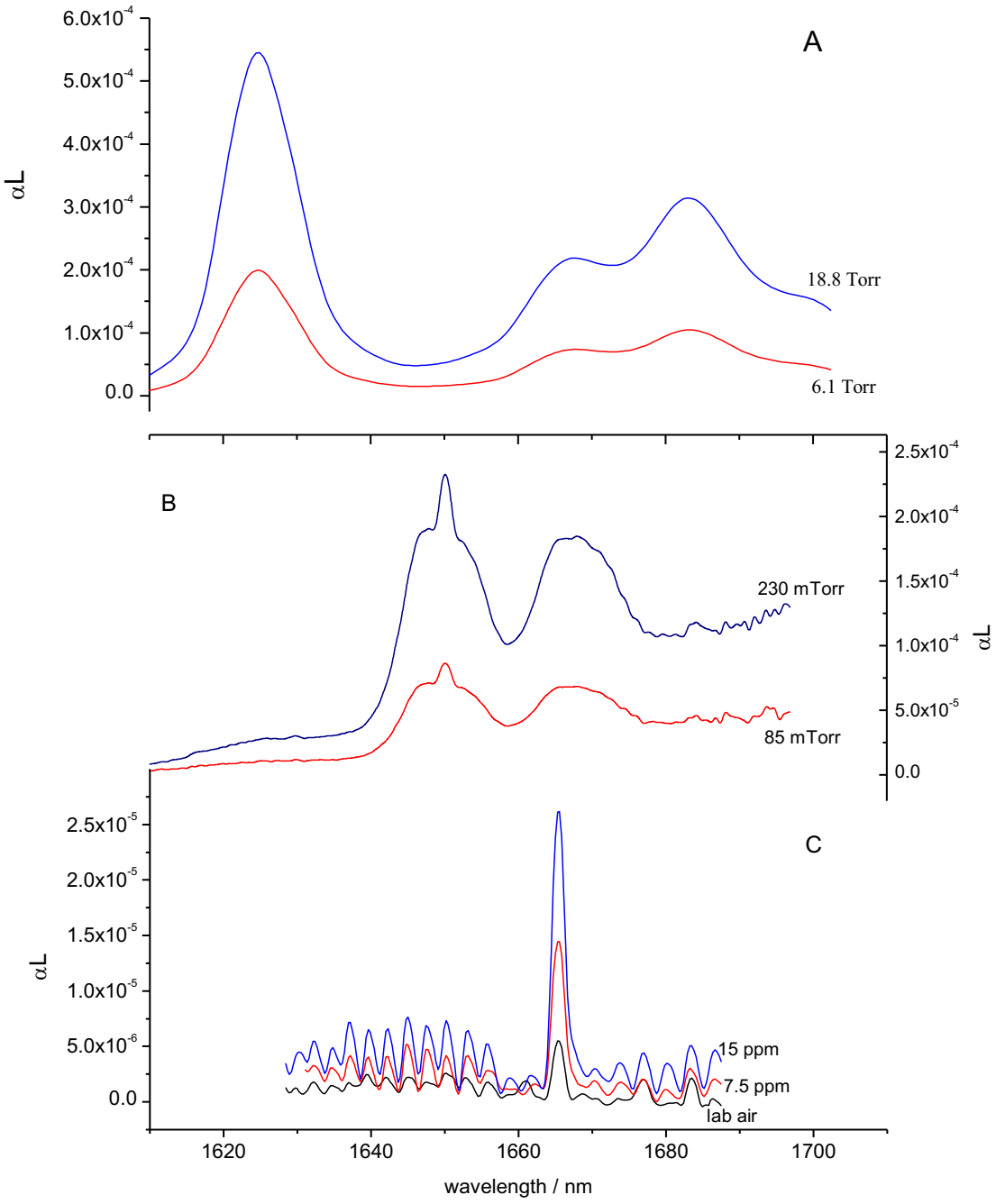
A
B
C
αL
6.0x10-4
5.0x10-4
4.0x10-4
3.0x10-4
2.0x10-4
1.0x10-4
0.0
18.8 Torr
6.1 Torr
2.5x10-4
2.0x10-4
1.5x10-4
1.0x10-4
5.0x10-5
230 mTorr
85 mTorr
2.5x10-5
2.0x10-5
1.5x10-5
1.0x10-5
5.0x10-6
15 ppm
7.5 ppm
lab air
1620
1640
1660
1680
1700
wavelength / nm

Figure 3

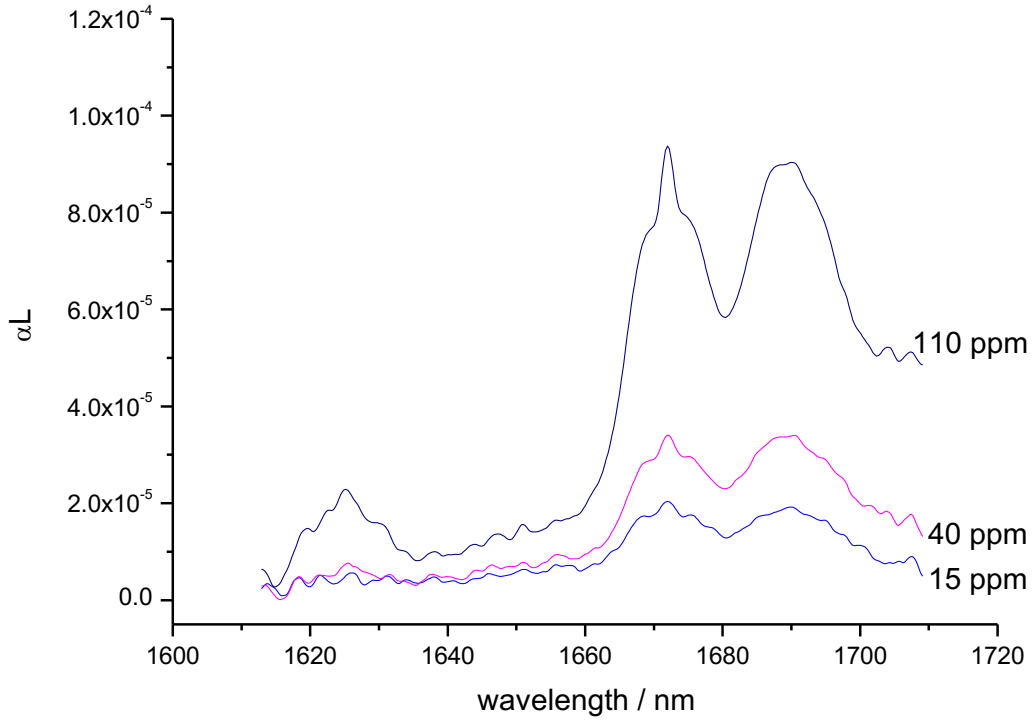
1.2x10-4
1.0x10-4
8.0x10-5
6.0x10-5
4.0x10-5
2.0x10-5
0.0
αL
1600
1620
1640
1660
1680
1700
1720
wavelength / nm
110 ppm
40 ppm
15 ppm

Figure 4

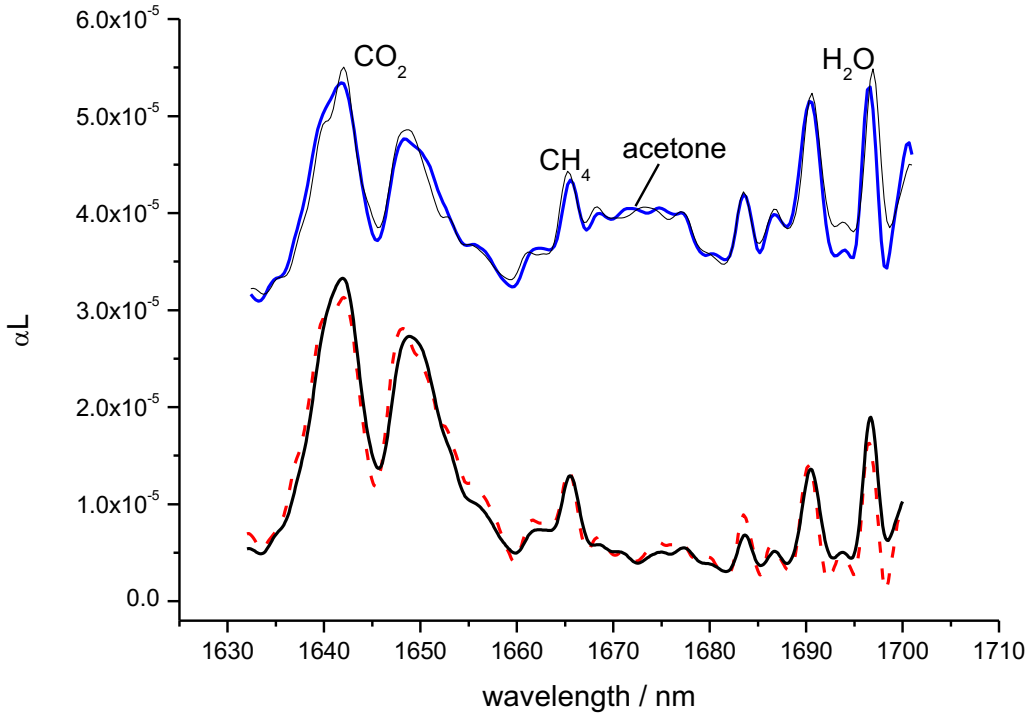
6.0x10-5
5.0x10-5
4.0x10-5
3.0x10-5
2.0x10-5
1.0x10-5
0.0
αL
CO2
CH4
acetone
H2O
1630
1640
1650
1660
1670
1680
1690
1700
1710
wavelength / nm

Figure 5

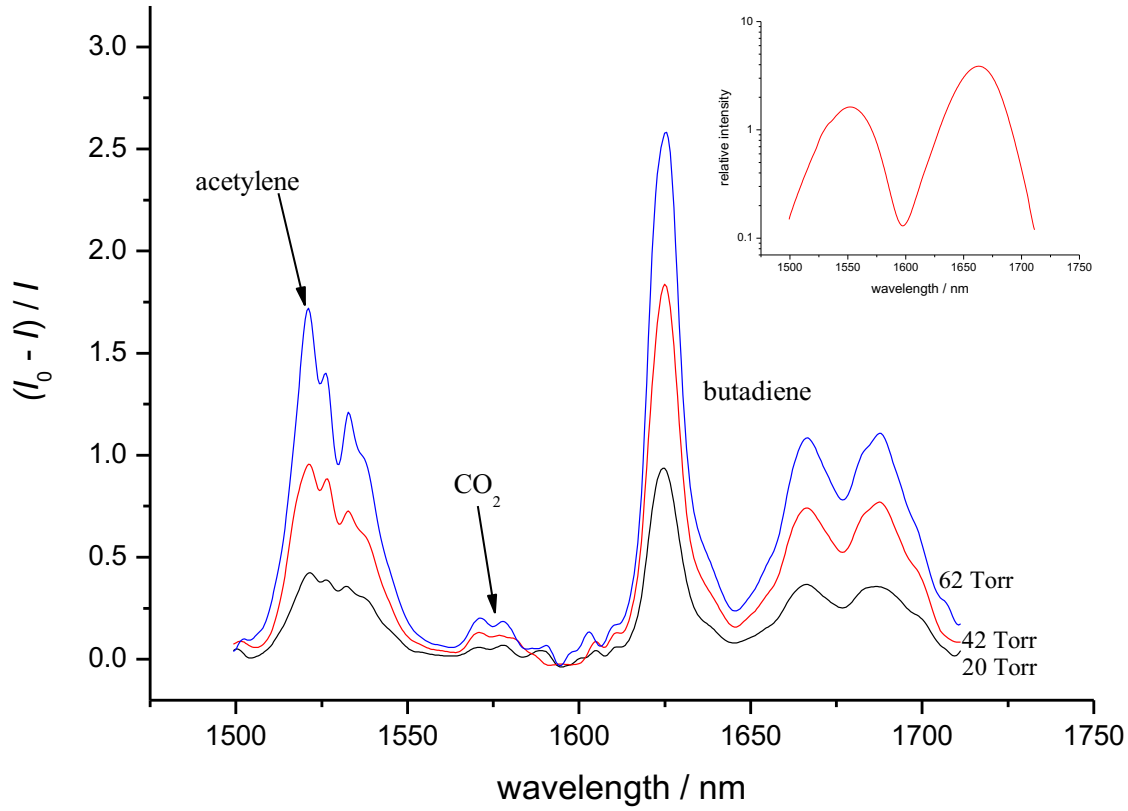
3.0
2.5
2.0
1.5
1.0
0.5
0.0
(I0 - I) / I
1500
1550
1600
1650
1700
1750
wavelength / nm
acetylene
CO2
butadiene
62 Torr
42 Torr
20 Torr
10
1
0.1
relative intensity
1500
1550
1600
1650
1700
1750
wavelength / nm